Electron energy-loss spectroscopy of V_2O_5 nanofibers synthesized by electro-spinning

D.M. Carrillo-Flores, M.T. Ochoa-Lara, F. Espinosa-Magaña

Abstract

The dielectric properties of V_2O_5 nanofibers, synthesized by the electrospinning method, are studied by analyzing the low-loss region of the electron energy loss spectroscopy (EELS) in a transmission electron microscope. A comparison of experimental EELS spectra and ab initio density-functional theory calcula-tions (WIEN2k code) within the Generalized Gradient Approximation (GGA) is presented, having found an excellent agreement between them. Although the experimental EELS has been acquired for the nanopar-ticles composing the fibers, and numerical calculations were carried out for bulk material, agreement between experimental and calculated results shows that no difference exists between the electronic structure in calculated bulk material and the nanoparticles. Furthermore, our results from EELS confirm that we accomplished the expected crystalline phase. The origins of interband transitions are identified in the electronic band structure by calculating the partial imaginary part of the dielectric function and the partial density of states.

Keywords: EELS, Ab initio, Dielectric function, V_2O_5, Nanofibers

Introduction

Vanadium oxides are of great interest in multiple applications, mainly because of the wide range of valency exhibited by V, which affects the physical and chemical properties of the oxides (Katzke et al., 2003; Schwingenschlögl and Eyert, 2004). Vanadium oxides can be used as catalysts (Gellings, 1985), e.g. for partial or selective

oxidation reactions. Furthermore, transitionmetal oxides, containing active sites able to adsorb gas molecules and catalyze reactions, are widely utilized as sensing elements in resistive gas sensors, especially those with d0 (e.g. V_2O_5) electron configurations (Wang and Chen, 2010; Shimizu et al., 2009). On the other hand, in commercial sensor devices, high gas sensitivity frequently requires high operating temperatures, which actually constitutes a significant drawback in terms of power consumption, cost and thermal stability (Wei et al., 2004; Santangelo et al., 2010; Ban and Whittingham, 2008; Wee et al., 2010). Therefore, great efforts are presently addressed to the development of materials allowing better sensor performances. For these purposes, divana-dium pentoxide (V_2O_5) has attracted great interest for its potential applications in numerous technological areas such as gas sensing, catalysis and electronics. V_2O_5 is an n-type semiconducting oxide whose electric conductivity increases when part of the V^{5+} species are reduced to V^{4+} because of the formation of oxygen vacancies. The sensing mechanism of most of the sensors for reducing gases exploits this property (Shimizu et al., 2009).

Nanotubes, nanowires, nanorods and nanobelts of V_2O_5 have been synthesized by different methods to maximize its surface area and to improve the sensing efficiency, such as sol–gel (Muster et al., 2000), reverse micelle (Pinna et al., 2003) and chemical vapor deposition (Wang et al., 2010). Recently, electro-spinning has been proposed as a novel technique for the low-cost preparation of one-dimensional transition-metal oxide based nanostructures (Viswanathamurthi et al., 2001; Guan et al., 2003; Kim et al., 2003; Faggio et al., 2011; Mai et al., 2010).

From a theoretical point of view, a number of first principles calculations have been carried out for V_2O_5, including electronic and mechanical properties (Reeswinkel et al., 2009; Brázdová et al., 2004; Hébert et al., 2002; Eyert and Höck, 1998).

On the other hand, electron energy-loss spectroscopy (EELS) has been widely used in the study of materials composition and electronic structure (Egerton, 1996; Ahn, 2004; Brockt and Lakner, 2000). The interactions of fast electrons with the specimen result in electrons being excited into unoccupied energy levels within the conduction band, as well as collective excitation of valence electrons. In the high-loss region, analysis of the first 10 eV of the spectra after the ionization edge (ELNES) can give information about the oxidation state, absolute energy position, and local symmetry via d level splittings in transition metal elements and orbital hybridization. The low-loss region can provide information about composition and electronic structure, and also the optical properties, although it has not been as widely applied as ELNES. This is due to the well-known fact that low-losses are caused by all possible transitions between the valence band and the conduction band. The valence band is made up of dispersed levels as opposed to almost flat core levels, and the interpretation of EELS is a priori more difficult.

From the dielectric theory, it is possible to relate the experimental single scattering distribution S(E), to the energy-loss function Im(−1/ε) (Egerton, 1996), by:

$$S(E) = \frac{I_0 t}{\pi a_0 m_0 v^2} Im\left[-\frac{1}{\varepsilon(q,E)}\right] \ln\left[1+\left(\frac{\beta}{\theta_E}\right)^2\right] \qquad (1)$$

where $\varepsilon(q,E) = \varepsilon_1 + i\varepsilon_2$ is the complex dielectric function at energyloss E and momentum transfer q,a_0 the Bohr radius, m_0 the electron rest mass, v the electron beam

velocity, θ the scattering angle and $\theta_E = E/(\gamma m_0 v^2)$ is the characteristic scattering angle, γ is the relativistic factor, I0 is the zero-loss intensity, t the specimen thickness, and β is the collection semi-angle. The real and imaginary parts of the dielectric function can be obtained from the energy-loss function through Kramers–Kronig analysis.

In this work, we studied the electronic structure of V_2O_5 nanofibers with both EELS, in the transmission electron microscope, and ab initio calculations with the FLAPW method, as implemented in WIEN2K code (Blaha et al., 1990, 2001). The aim is to determine the dielectric properties of V_2O_5 nanofibers, via valence electron energy-loss spectroscopy (VEELS) and to compare with ab initio calculations. Even though there are many articles studying the high energy-loss EELS of V_2O_5 (Pinna et al., 2003; Su et al., 2001; Ding et al., 2008; Grogger et al., 2008; Mitterbauer et al., 2003) in the literature, we were not able to find any references addressing low energy-loss EELS. Our focus rests on the electronic structure of V_2O_5 nanoparticles composing the fibers.

Experimental

The synthesis of the V_2O_5 nanofibers was carried out by the electro-spinning method. A detailed description of the procedure can be found in the literature (Faggio et al., 2011; Li and Xia, 2004; Chronakis, 2005). In this work, the precursor solution was composed of poly(vinylpyrrolidone) (PVP), with molecular weight MW 1,300,000, and vanadyl sulfate ($VOSO_4$), dissolved in ethanol. The solution was heated at 60 °C with vigorous stirring for 4 h and then delivered into a metallic needle at a constant flow rate of 0.3 mL/h by a syringe pump. The metallic needle was connected to a high-voltage power supply and a grounded aluminum foil was placed 15 cm from the needle tip. With an applied high-voltage of15 kV, the precursor solution jet was accelerated toward the

aluminum foil, leading to the formation of $VOSO_4$/PVP fiber composite, together with a rapid evaporation of the ethanol. The composite nanofibers were then annealed at 600 °C for 1 h, with a slope of 3 °C/min to obtain V_2O_5 nanofibers.

The thermal stability of as-spun and calcined PVP-$VOSO_4$ fibers was analyzed by thermogravimetry–differential scanning calorimetry (TG–DSC) using a TA Instruments Q600 thermal analyzer at a heating rate of 3 °C/min under inert atmosphere with 50 cm^3/min of argon flux.

X-ray diffraction (XRD) measurements were performed in a Panalytical diffractometer with Cu Kα radiation(1.54060). For XRD measurements, the nanofibers were separated from the aluminum foil and then slightly pressed on a glass slide to form a dense film.

Field-emision scanning electron microscopy (FESEM) images were acquired with a JEOL JSM-7401F at an accelerating voltage of 10 kV. High-resolution transmission electron microscopy (HRTEM) images were recorded by using a JEOL JEM-2200FS microscope.

Electron energy-loss spectra were obtained using a Gatan parallel electron energy-loss spectrometer (PEELS model 766) attached to a transmission electron microscope (TEM) Philips CM200. Spectra were acquired in diffraction mode with 0.2 eV/channel dispersion, an aperture of 2 mm, and a collection semi-angle of about 4 mrad. The resolution of the spectra was determined by measuring the full-width at half-maximum (FWHM) of the zero-loss peak, and this was typically close to 1.0 eV, when the TEM was operated at 120 kV. EELS spectra were corrected for dark current and readout noise. The channel to channel gain variation was minimized by normalizing the

experimental spectrum with independently obtained gain spectrum from the spectrometer. Next, spectra were Fourierlog deconvoluted to have the single scattering distributions S(E), by using the program FLOG (Egerton, 1996). The real and imaginary parts of the dielectric function can be obtained from the energy-loss function $\mathrm{Im}(-1/\varepsilon)$ (Eq. (1)) through the Kramers–Kronig analysis. Theoretically, by measuring the absolute cross section and the thickness of the sample, we can obtain the value of the energy-loss function. However, this approach is usually not practically feasible. In order to obtain the absolute value of the energy-loss function for semiconductor materials, the refractive index at one point is needed to normalize the energy-loss spectra. We have used the value of 2.28, taken from the literature (Kaid, 2006) and then the program KRAKRO (Egerton, 1996) to obtain the dielectric function.

Calculation details

Self-consistent band structure calculations were performed using density-functional theory (DFT) with the full-potential linearized augmented plane-wave (FLAPW) method, using the WIEN2k code (Blaha et al., 2001). Exchange and correlation were treated using the generalized gradient approximation (GGA) for the potential. The core states were treated in a fully relativistic fashion. The wave functions within the muffin-tin spheres were expanded in spherical harmonics with an angular momentum up to l = 10. Additional local orbital extensions were used to avoid linearization errors. Nonspherical contributions to the charge density and the potential within the muffin-tin spheres were considered up to l_{max} = 4. In the interstitial region, plane waves with reciprocal lattice vectors up to G = 10 were included, and the plane-wave cut-off (RMTKmax) was set to 7. Self-consistency was considered to be achieved

when the total energy variation from iteration to iteration did not exceed 10^{-6} Ry, on a mesh containing 396 k-points in the irreducible Brillouin zone (IBZ).

The dielectric function can be obtained from the Optic Program of the WIEN2k code (Ambrosch-Draxl and Soto, 2006), allowing for comparison with experiment:

$$\varepsilon_{2ii}(\omega) = \frac{4\pi^2 e^2}{m^2\omega^2 V}\sum_{v,c,k}|\langle\psi_k^v\left|p_i\right|\psi_k^c\rangle|^2 \times \delta(E_{\psi_k^c} - E_{\psi_k^v} - \hbar\omega) \qquad (2)$$

Matrix elements are calculated from the electron states and integration over the irreducible Brillouin zone is performed to calculate the imaginary part of the dielectric function. Then a Kramers–Kronig analysis is performed to obtain the real part of the dielectric function ε1, and finally, the energy-loss function Im(−1/ε).

The crystal structure of V_2O_5 has been widely studied experimentally. The structure belongs to the space group Pmmn. The lattice constants are a = 11.5219, b = 3.5667, c = 4.3751Å, taken from the experimental results (Haas et al., 2003). The atomic positions are: V at (0.1010, 0.250, 0.8967) and three non-equivalent oxygen atoms at (0.1077, 0.250, 0.5333), (0.9297, 0.250, 0.5333) and (0.250, 0.250, 0.9920). The optical properties were calculated on a mesh containing 1920 k-points in the irreducible part of the Brillouin zone, as many points are needed for optical calculations.

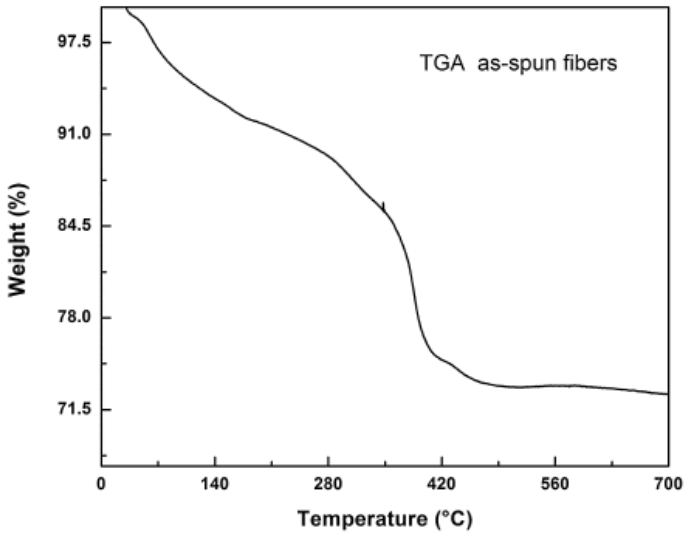

Fig. 1. TGA analysis of as-spun $VOSO_4$/PVP fiber composite.

Results and discussion

To choose the most suitable range of calcination temperature of the as-spun fibers, their thermal stability was investigated by thermogravimetric analysis (TGA), as shown in Fig. 1. The TGA profile reveals that evaporation of residual molecules of ethanol is responsible for the mass loss at T < 100 °C. Above this temperature and up to about 400 °C, evaporation of the polymer takes place, and at T < 500 °C, evaporation of the residual sulfur leaves only vanadium oxide. On this basis, we choose 600 °C as a suitable temperature for calcinations of the as-spun fibers.

The presence of pure orthorhombic phase of V_2O_5 is confirmed by XRD analysis. Fig. 2 shows the amorphous structure (as-spun), calcined (V_2O_5 fibers) and reference data, showing the formation of crystalline divanadium pentoxide. Diffraction-peak identification is performed on the basis of the PDF2 release 2010 ICDD database, card number 00-041-1426.

Fig. 3a shows SEM micrographs of as-spun fibers. Cylindrical and randomly oriented fibers were obtained with diameter about 100–500 nm. Fig. 3b shows the morphology of V2O5 fibers after calcinations at 600 °C. The diameter shows a greater dispersion than the as-spun fibers, indicating that fibers agglomerate after calcination.

Fig. 4a–d shows TEM micrographs from an isolated, calcined V_2O_5 nanofiber, after dispersing the sample in isopropanol. Fig. 4a shows a bent V-shaped fiber about 5 μm long. Fig. 4b shows the same fiber at higher magnification, where the nanoparticles composing the fiber are clearly seen. Fig. 4c and d shows the interface between two adjacent nanoparticles. Well defined planes are observed, indicating a good crystallinity of the nanoparticles.

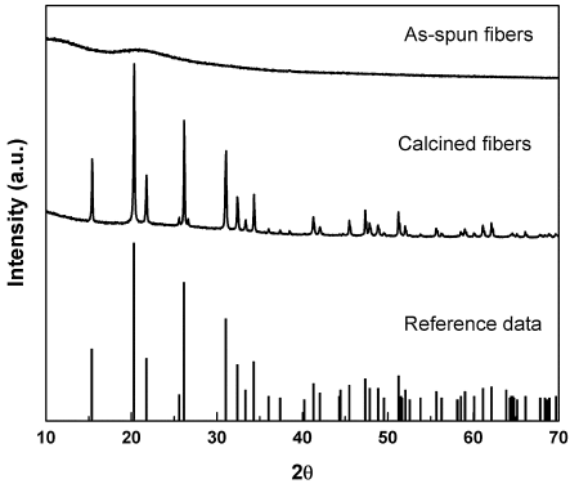

Fig. 2. XRD patterns of as-spun and calcined $VOSO_4$/PVP composite.

Original EELS spectrum, acquired on a single nanocrystal, is shown in Fig. 5, prior to extracting the single scattering distribution. Fig. 6 shows the EELS-derived energy-loss function Im(−1/ε) of the nanoparticles forming the nanofibers, as well as calculated for bulk V_2O_5, where a Lorentzian broadening with 0.5 eV has been applied to the later. EELS spectra were acquired on nanoparticles of several sizes and no

changes were found in the energy loss function. In anisotropic materials, dielectric properties must be described by the dielectric tensor; however, for the interpretation of EELS spectra acquired from a polycrystalline sample, the differential inelastic scattering cross section is averaged over all angles, therefore, the reported calculated dielectric function is an “effective dielectric function”, that can be written as $\varepsilon_{eff} = (\varepsilon_{xx} + \varepsilon_{yy} + \varepsilon_{zz})/3$.

Comparison between experimental and calculated spectra is quite good indeed, even though some features in experimental spectrum are missing, which can be attributed to the relatively low energy resolution attained in experimental results (~1.0 eV). Even though we acquired EELS spectra from the V_2O_5 nanoparticles composing the fibers, and numerical calculations were carried out for the bulk material, the match between experimental and calculated spectra leads us to conclude that the electronic structure of the nanoparticles exhibits no discrepancy with that of the bulk sample, at least within our experimental resolution. Differences seem to appear at smaller sample size, as reported previously for other structures (Morales-Rodríguez and Espinosa-Magaña, 2012).

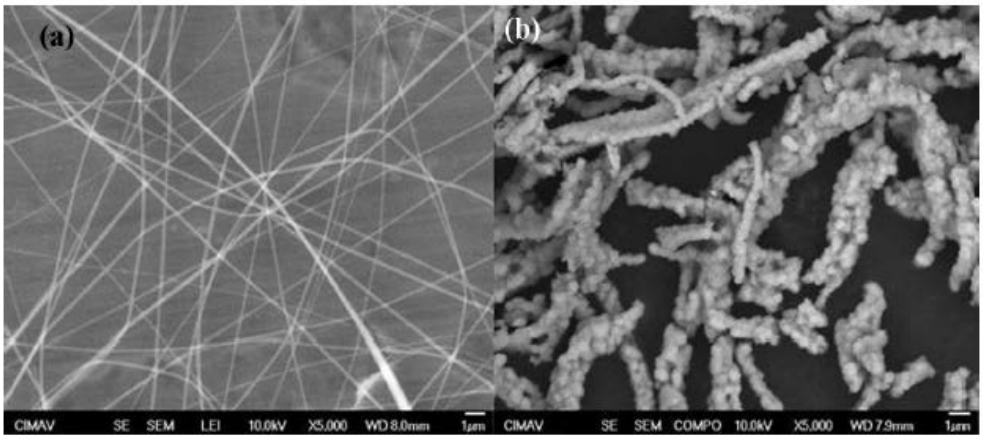

Fig. 3. SEM images of as-spun and calcined $VOSO_4$/PVP composite.

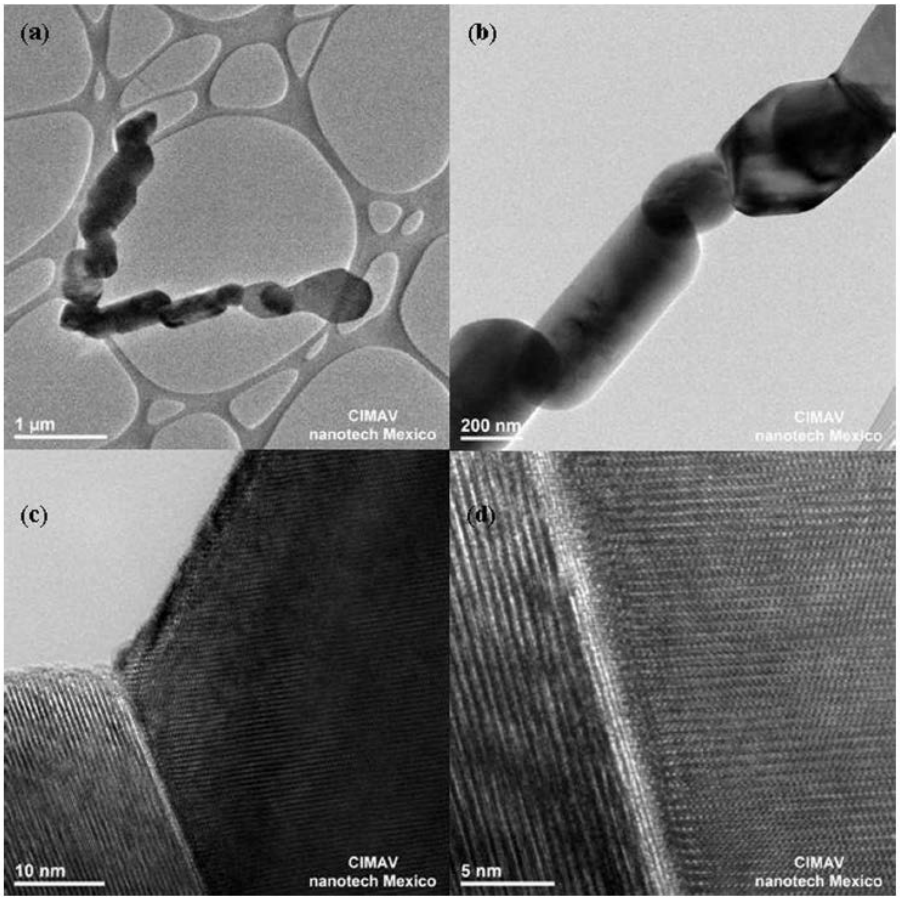

Fig. 4. TEM images of V_2O_5 nanofibers, at different magnifications.

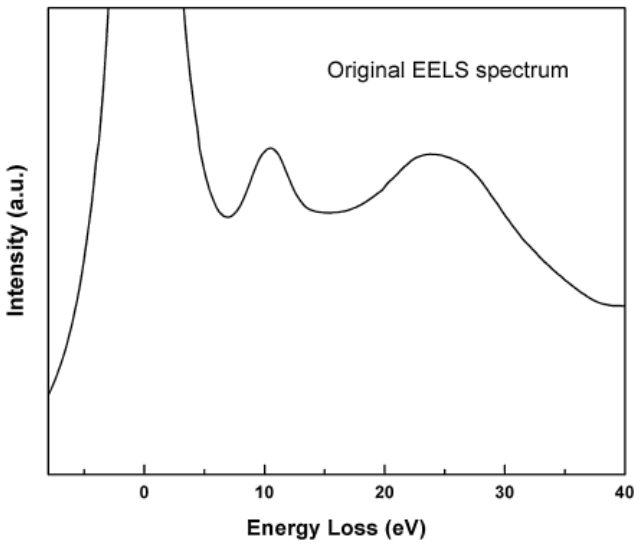

Fig. 5. Original EELS spectrum of V_2O_5 nanofibers, without zero-loss peak removed.

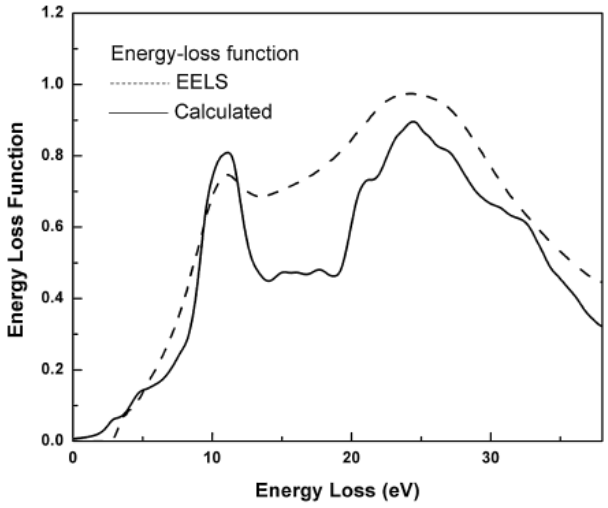

Fig. 6. Calculated (-) and EELS-derived (- - -) energy-loss function of V_2O_5 nanofibers.

For the analysis, numerical calculations prove to be of paramount aid in the interpretation of EELS spectra, given the high resolution that can be attained through said calculations.

Well defined maxima can be observed in calculated energy-loss spectrum at 2.9, 4.8, 7.7, 11.2, 15.2, 17.7, 21.0 and 24.4 eV. Peak at 11.1 eV is a plasmon resonance, as can be confirmed by Fig. 7, which shows the real part of the dielectric function, where we have identified the point which has zero-crossing with the energy axis with a positive slope, indicating the presence of a well-defined plasmon signal at 10.1 eV. The other maxima in the energy-loss function arise from interband transitions, as observed in Fig. 8, as peaks in the imaginary part of the dielectric function ε_2, at 2.8, 4.1, 6.3, 14.6, 17.4, 19.5 and 22.0 eV. The origin of these peaks can be sought after by calculating the partial imaginary part of the dielectric function, as implemented in WIEN2k.

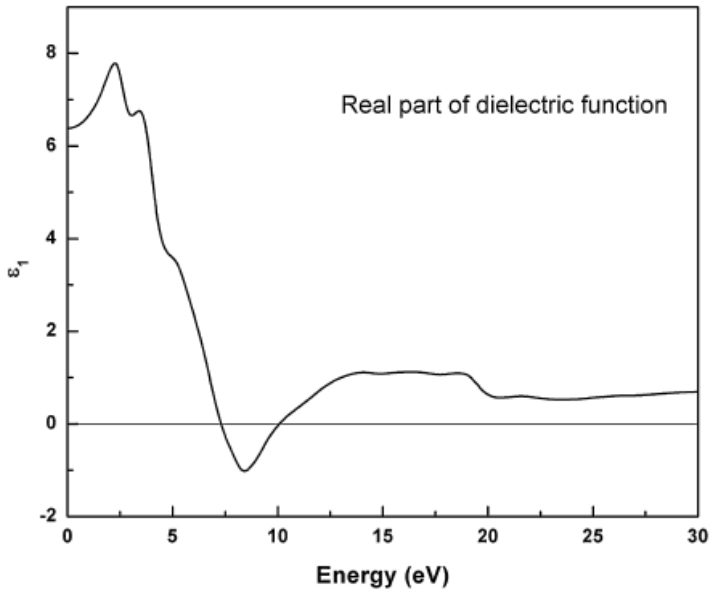

Fig. 7. Calculated real part of the dielectric function, ε_1, of V_2O_5 nanofibers.

This allows using a smaller set of energy-bands from where the construction of the partial ε_2 could be made up and which arises from all possible combinations of the valence and conduction bands of the chosen set (Launay et al., 2004; Gallegos-Orozco et al., 2008). With the aid of the calculated total and angular-momentum and site decomposed density of states (DOS), shown in Fig. 9, we can identify maxima in the ε2 vs E plot as interband transitions. Since there are three non-equivalent oxygen atoms in the unit cell, we chose to plot the sum of the density of states for oxygen in Fig. 9.

If we consider that only dipole transitions are allowed, maxima at 2.8 and 4.1 eV arise mainly by transitions from O 2p to V 3d states, peak at 6.3 eV originates from transitions between O 2p states in the valence band and V 3d and O 3s states in conduction bands, peaks at 14.6 and 17.4 eV come mainly from transitions between O 2p and O 4s states, peak at 19.5 eV originates by transitions from V 3s to V 4p and O

3p states and, finally, maximum at 22.0 eV comes from transitions between O 2p and V 4s states.

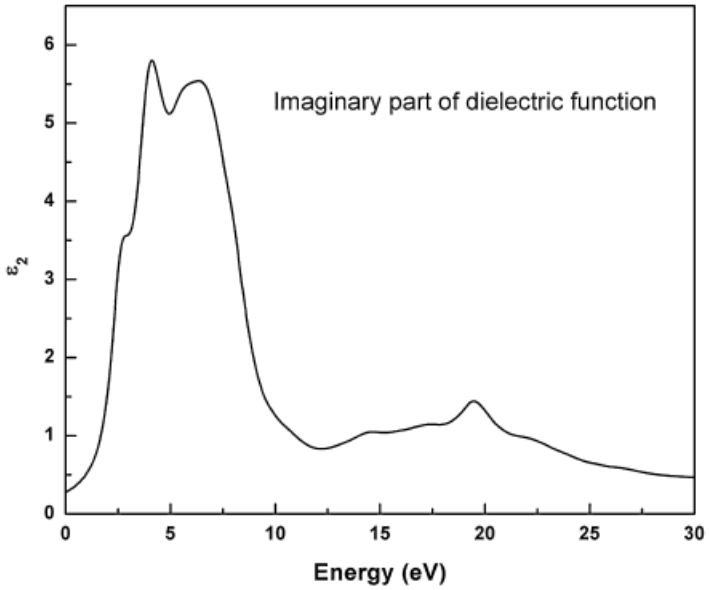

Fig. 8. Calculated imaginary part of the dielectric function, ε_2, of V_2O_5 nanofiber

Conclusions

The dielectric properties of V_2O_5 nanofibers, synthesized by the electrospinning method, have been studied by low-loss transmission electron energy loss spectroscopy and ab initio calculations. Excellent agreement has been found between experimental and calculated spectra, taking into account the relatively low resolution attained in EELS spectra (~1 eV). The match between experimental energy loss function and numerical calculations shows that there are no differences between the electronic structure of V_2O_5 of the bulk material and that of the nanoparticles, at least within our experimental resolution. Changes in the dielectric properties, and thus in the electronic structure, seem to appear at smaller sample size.

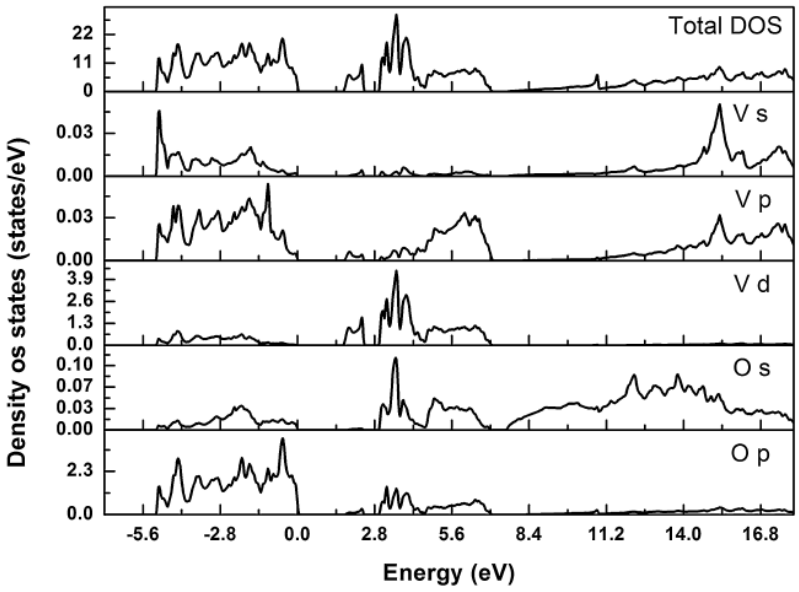

Fig. 9. Calculated total and partial site-projected density of states of V_2O_5 nanofibers. The Fermi energy has been chosen at the origin.

From the calculated energy loss function and the imaginary part of the dielectric function, we were able to identify the plasmon energy, as well as interband transitions in a band structure picture. This way, numerical calculations are a valuable tool for the interpretation of EELS spectra.

Acknowledgements

The technical support of Carlos Ornelas, Raúl Ochoa, Wilber Antunez, Enrique Torres and Daniel Lardizábal is greatly appreciated. One of the authors (D.M. Carrillo-Flores) gratefully acknowledges the support by grants from CONACYT, México.

References

1.-Ahn, C.C., 2004. Transmission Electron Energy Loss Spectrometry in Materials Science and the EELS Atlas. WILEY-VCH Verlag GmbH & Co., KGaA, Weinheim.

2.- Ambrosch-Draxl, C., Soto, J.O., 2006. Linear optical properties of solids within the full-potential linearized augmented planewave method. Computer Physics Communications 175, 1–14.

3. - Ban, C., Whittingham, M.S., 2008. Nanoscale single-crystal vanadium oxides with layered structure by electrospinning and hydrothermal methods. Solid State Ionics 179, 1721–1724.

4. - Blaha, P., Schwarz, K., Madsen, G.K.H., Kvasnicka, D., Luitz, J., 2001. Computer code WIEN2k. Technische Universität Wien, Austria, 2001.

5. - Blaha, P., Schwarz, K., Sorantin, P., Trickey, S.B., 1990. Comput. Improved version of P. Blaha, K., Schwarz, P. Sorantin and S.B. Trickey. Computer Physics Communications 59, 399.

6.- Brázdová, V., Ganduglia-Piranno, M.V., Sauer, J., 2004. Periodic density functional study on structural and vibrational properties of vanadium oxide aggregates. Physical Review B 69, 165420.

7. - Brockt, G., Lakner, H., 2000. Nanoscale EELS analysis of dielectric function and bandgap properties in GaN and related materials. Micron 31, 435–440.

8.- Chronakis, I.S., 2005. Novel nanocomposites and nanoceramics based on polymer nanofibers using electrospinning process – a review. Journal of Materials Processing Technology 167, 283–293.

9.- Ding, N., Liu, S., Chen, C., Lieberwirth, I., 2008. An electron microscopic investigation of structural variation of V_2O_5 fibers after working as ethanol sensors. Applied Physics Letters 93, 173510–182008.

10.- Egerton, R.F., 1996. Electron energy Loss Spectroscopy in the Electron Microscope. Plenum Press, New York.

11.- Eyert, V., Höck, K.H., 1998. Electronic structure of V_2O_5: role of octahedral deformations. Physical Review B 57, 12727.

12.- Faggio, G., Modafferi, V., Panzera, G., Alfieri, D., Santangelo, S., 2011. Micro-Raman and photoluminescence analysis of composite vanadium oxide/poly-vinyl acetate fibres synthesised by electro-spinning. Journal of Raman Spectroscopy 42, 593–602.

13.- Gallegos-Orozco, V., Martínez-Sánchez, R., Espinosa-Maga˜na, F., 2008. In situ char-acterization of the ferroelectric transition in BaTiO3 by EELS and comparison with ab initio methods. Physical Review B 77, 045128.

14.- Gellings, P.J., 1985. In: Webb, G., Bond, G.C. (Eds.), Catalysis, vol. 7. The Royal Society of Chemistry, London.

15.- Grogger, W., Hofer, F., Kothleitner, G., Schaffer, B., 2008. An introduction to high-resolution EELS in transmission electron microscopy. Topics in Catalysis 50,200–207.

16.- Guan, H., Shao, C., Wen, S., Chen, B., Gong, J., Yang, X., 2003. A novel method forpreparing Co_3O_4nanofibers by using electrospun PVA/cobalt acetate compositefibers as precursor. Materials Chemistry and Physics 82, 1002–1006.

17.- Haas, F., Adams, A.H., Buhrmester, T., Schimanke, G., Martin, M., Fuess, H., 2003. X-ray absorption and X-ray diffraction studies on molybdenum doped vanadiumpentoxide. Physical Chemistry Chemical Physics 5, 4317–4324.

18.- Hébert, C., Willinger, M., Su, D.S., Pongratz, P., Schattschneider, P., Schlögl, R., 2002.Oxygen K-edge in vanadium oxides: simulations and experiments. EuropeanPhysical Journal B 28, 407–414.

19.- Kaid, M.A., 2006. Characterization of electrochromic vanadium pentoxide thin filmsprepared by spray pyrolysis. Egyptian Journal of Solids 29, 273–291.

20.- Katzke, H., Tolédano, P., Depmeier, W., 2003. Theory of morphotropic transformations in vanadium oxides. Physical Review B 68, 024109.

21.- Kim, H.Y., Viswanathamurthi, P., Bhattarai, N., Lee, D.R., 2003. Vanadium oxidenanofibers by electrospinning. Advances in Materials Science 5, 216–219.

22.- Launay, M., Boucher, F., Moreau, P., 2004. Evidence of a rutile-phase characteristicpeak in low-energy loss spectra. Physical Review B 69, 035101.

23.- Li, D., Xia, Y., 2004. Electrospinning of nanofibers: reinventing the wheel?? AdvancedMaterials 16, 1151–1170.

24.- Mai, L., Xu, L., Han, C., Xu, X., Luo, Y., Zhao, S., Zhao, Y., 2010. Electrospun ultralonghierarchical vanadium oxide nanowires with high performance for lithium ionbatteries. Nano Letters 10, 4750–4755.

25.- Mitterbauer, C., Kothleitner, G., Grogger, W., Zandbergen, H., Freitag, B., Tiemeijer, P.,Hofer, F., 2003. Electron energy-loss near-edge structures of 3d transition metaloxides recorded at high-energy resolution. Ultramicroscopy 96, 469–480.

26.- Morales-Rodríguez, H.J., Espinosa-Magaña, F., 2012. Experimental and theoretical determination of the low-loss electron energy loss spectroscopy of nanostruc-tured ZnO. Micron 43, 177–182.

27.- Muster, J., Kim, G.T., Krstic, V., Park, J.W., Roth, S., Burghard, M., 2000. Electrical trans-port through individual vanadium pentoxide nanowires. Advanced Materials 12,420.

28.- Pinna, N., Wild, U., Urban, J., Schlögl, R., 2003. Divanadium pentoxide nanorods.Advanced Materials 15, 329–331.

29.- Santangelo, S., Messina, G., Faggio, G., Willinger, M.G., Pinna, N., Donato, A., Arena, A.,Donato, G., Neri, G., 2010. Micro-Raman investigation of vanadium-oxide coatedtubular carbon nanofibers for gas-sensing applications. Diamond and RelatedMaterials 19, 590–594.

30.- Reeswinkel, T., Music, D., Schneider, J.M., 2009. Ab initio calculations of the structureand mechanical properties of vanadium oxides. Journal of Physics: CondensedMatter 21, 145404.

31.- Schwingenschlögl, U., Eyert, V., 2004. The vanadium magnéli phases V_nO_{2n-1}.Annalen der Physik 13, 475–510.

32.- Shimizu, K.I., Chinzei, I., Nishiyama, H., Kakimoto, S., Sugaya, S., Matsutani, W.,Satsuma, A., 2009. Doped-vanadium oxides as sensing materials for high tem-perature operative selective ammonia gas sensors. Sensors and Actuators B 141,410–416.

34.- Su, D.S., Wieske, M., Beckmann, E., Blume, A., Mestl, G., Schlögl, R., 2001. Electronbeam induced reduction of V_2O_5studied by analytical electron microscopy.Catalysis Letters 75, 81–86.

35.- Viswanathamurthi, P., Bhattarai, N., Kim, H.Y., Lee, D.R., 2001. Vanadium pentoxidenanofibers by electrospinning. Scripta Materialia 49, 577–581.

36.- Wang, C.T., Chen, M.T., 2010. Vanadium-promoted tin oxide semiconductor carbonmonoxide gas sensors. Sensors and Actuators B 150, 360–366.

37.- Wang, Y., Su, Q., Chen, C.H., Yu, M.L., Han, G.J., Wang, G.Q., Xin, K., Lan, W., 2010. Lowtemperature growth of vanadium pentoxide nanomaterials by chemical vapourdeposition using $VO(acac)_2$ as precursor. Journal of Physics D: Applied Physics43, 185102.

38.- Wee, G., Soh, H.Z., Cheah, Y.L., Subodh, G., 2010. Synthesis and electrochemical prop-erties of electrospun V_2O_5nanofibers as supercapacitor electrodes. Journal ofMaterials Chemistry 20, 6720–6725.

39.- Wei, B.Y., Hsu, M.C., Su, P.G., Lin, H.M., Lai, R.J.W.J., 2004. A novel SnO2gas sen-sor doped with carbon nanotubes operating at room temperature. Sensors andActuators B 101, 81–89.